Digest Journal of Nanomaterials and Biostructures Vol. 13, No. 1, January - March 2018, p. 253 - 261

EFFECT OF CLUSTERING ON THE MECHANICAL PROPERTIES OF SiC_P REINFORCED ALUMINUM METAL MATRIX COMPOSITES

X. M. DU*, K. F. ZHENG, F. G. LIU
School of Materials Science and Engineering, Shenyang Ligong University, Shenyang 110159, China

This paper reports an aluminum matrix composite reinforced with SiC particle (SiC_p/Al) using the ball-milling and hot-press sintering. The effects of SiC_p content and ball-milling time on microstructure and mechanical properties of the composites were investigated using scanning electron microscopy (SEM), X-ray diffraction (XRD) and tensile tests. Microstructural investigation shows that the micro-sized SiC particles had been dispersed homogeneously in the aluminum matrix when the content of SiC_p is up to 2.5 wt%. However, the particle agglomeration is observed in the composite when the SiC_p content is above 3.5 wt%. The composite with 2.5 wt% SiC_p content exhibits a highest tensile strength and hardness in which the improvement is 41.5 % and 25.86 %, respectively, over unreinforced aluminum matrix. But the elongation decreases with increasing the content of the SiC_p, indicating that increasing the content of the SiC_p degrade the plasticity of the composites. The fracture mechanism of the composites changes from ductile to brittle with the increase in the content of the SiC_p.

(Received October 26, 2017; Accepted February 22, 2018)

Keywords: Aluminum matrix composites; SiC particle; Powder metallurgy; Mechanical properties.

1. Introduction

Aluminum matrix composites with SiC_p reinforcement are the materials in which aluminum is used as matrix material reinforced with SiC_p. SiC_p reinforced aluminum matrix composites have a numerous applications in aerospace, ground and water transportation applications like in airframes, pistons, submarine etc., because of their lower density, higher specific strength, better physical and mechanical properties [1,2].

In recent years, the SiC_p reinforced aluminum matrix composites are gaining importance because of their low cost with advantages like isotropic properties and the possibility of secondary processing facilitating fabrication of secondary components [3]. However, there are some problems that are not resolved, restricting the application of composite materials. A major potential problem in the application of SiC_p/Al composites is the possibility that the reaction between Al and SiC produces Al_4C_3, which weakens the interface depending on the temperature, environment, and other parameters. Lai and Chung [4] noticed that SiC reacts with Al at higher temperature and forms aluminum carbide in stir casting process, and they proposed surface modification techniques to avoid direct contact between matrix and reinforcement. The other problem of SiC/Al composites is that the microstructure is non-uniform with elongated clusters of particles present along the extrusion direction. The most significant detrimental property change may be the decrease in ductility and fracture toughness, which is true for all the aluminum matrix composites.

Many researchers found that composites manufactured specifically by liquid methods such as stir casting suffer from particle pushing, resulting in rejection and agglomeration of particles

* Corresponding author: du511@163.com

from the growing solid/liquid interface during solidification [5-8]. It induces the agglomeration and clustering of the particles in the matrix, prompting low tensile properties, especially ductility, associated with intergranular fracture mode in the final solidified material. Undoubtedly, the powder metallurgy (PM) technique has been a prominent method to resolve the problems on the agglomeration of particles and undesirable chemical reaction at the interface for composites processing.

The principal objective of this current investigation was to determine how the preparing parameters, such as the ball-milling time and particle mass fraction, affect the distribution of SiC_p in aluminum matrix. Another objective was to shed more light on the extent of particles clustering in the composites so as to aid in the correlation between microstructure and tensile properties of SiC_p/Al composites.

2. Experimental procedure

2.1 Materials

Atomized pure aluminum powder (Anshan Steel Industrial Fine Aluminum, Inc., China) with an average size of 10 um and chemical composition (Fe 0.071 wt.%, Si 0.067 wt.%, Cu 0.002 wt.%) was used as matrix material. The α-SiC particles of 2um with green color was reinforced in the matrix material.

2.2 Composites preparation

A planetary machine was used for ball milling without interruption under high purity (99.999%) argon gas. The stainless steel vial was sealed with an elastomeric O ring. The ZrO_2 balls to powder weight ratio was 7:1, and the rotation rate of the vial was 40 rpm under a total milling time of 18, 24 and 30 h, respectively.

SiC particles were incorporated into the matrix material in 1.5 wt.%, 2.5 wt.%, 3.5 wt.% and 4.5 wt.% mass fractions. The ball-milled powder was containerized in a heat-resisting steel die (50 mm in diameter, 200 mm in height, and 10 mm in thickness), then compacted. The compacted composite billets were sintered at 610 °C for 3 hours under a pressure of 30 MPa by hot-press sintering. For comparison, a pure Al sample was also fabricated under the same conditions.

2.3 Characterization

X-ray diffraction analysis on polished sintered sample bars were carried out by X-ray diffractometer (Rigaku Ultima IV), using Cu K_α radiation for 20-90 degrees. Raw XRD data were refined and analyzed via MDI Jade 6.0 program (Materials Data Incorporated: Livermore, CA, USA). The surface morphology was observed by a scanning electron microscopy (SEM) of S-3400N equipped with energy-dispersive spectrometer (EDS) and an optical microscope of Carl Zeiss Axioert200MAT.

Hardness measurements of composite samples were carried out on a Vickers hardness testing machine (Shanghai Shuangxu, Inc., HVS-50, China), using a load of 9.8 N, and the mean values of at least five measurements conducted on different areas of each sample was considered.

The tensile properties of the sintered samples with dimensions of 20 mm×10 mm×2.0 mm were determined by a testing machine (UTM4304, Shenzhen Suns Technology Stock Co., Ltd, China) at ambient temperature using a displacement rate of 0.01 mm/s.

3. Results and discussion

3.1. Microstructure

Fig. 1 shows the images from SEM of pure aluminum powder and SiC particles. The particle shape of aluminum is regularly spheroidal. The mean size of the particles appears to be ~ 10um with some smaller particles of 3-4 um and some larger particles of about 15 um (Fig.1 (a)). The SiC particles with an average particle size of 2 ìm, as shown in Fig.1(b).

The example of powder structure evolution versus ball milling time for 2.5 wt%-SiC_p/Al

composite has been highlighted in Fig. 2. A visible plastic deformation is observed in several particles, which present a flaky morphology, in samples beyond 24 h of milling (Fig. 2 (c) – (d)). Similar observations were found in previous studies [9,10]. During ball milling, the particles go through the following processes, such as plastic deformation, cold welding, fracture and these repeated processes. The plastic deformation causes flattening of the particles. The SiCp were found mainly among the flat Al particles (Fig. 2 (a) and (b)). After being mixed for 24 h, the powder morphology transfers from the spherical powder to flaky shape. The further plastic deformation results in cold welding of the particles. An increase in particle size is observed. In addition, many SiC particles were enclosed between the flaky particles when they were aggregated into lamellar structures through cold welding (Fig. 2 (c) and (d)). As a consequence of the increase in the number of impacts of powders by the milling media, the fracture of the cold welding particles occurs. The process is repeated. Eventually, the equilibrium state between fracture and welding of particles is achieved. It is important to notice that the aggregation of SiC_p disappears for 2.5 wt%-SiC_p/Al powder at milling time of 24 h (Fig. 2 (c)). It indicates an excellent dispersion of the SiC_p in the aluminum matrix in short periods of milling time by using ball milling. Longer milling times have no obvious improvement for the dispersion of SiC_p in aluminum matrix (Fig. 2 (d)). The ball milling time is determined to be 24 hours in this experiment.

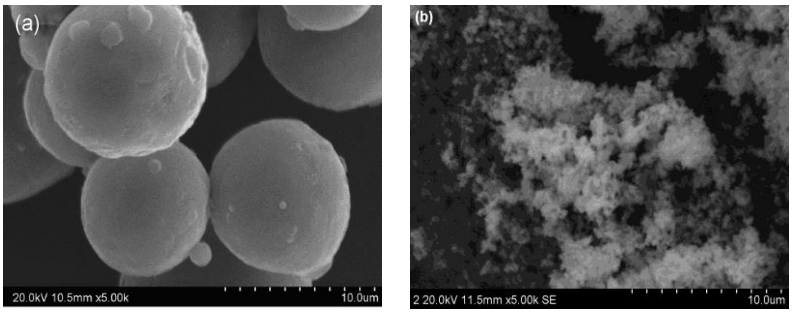

Fig. 1. SEM morphology of (a) pure aluminum and (b) SiC_p powders.

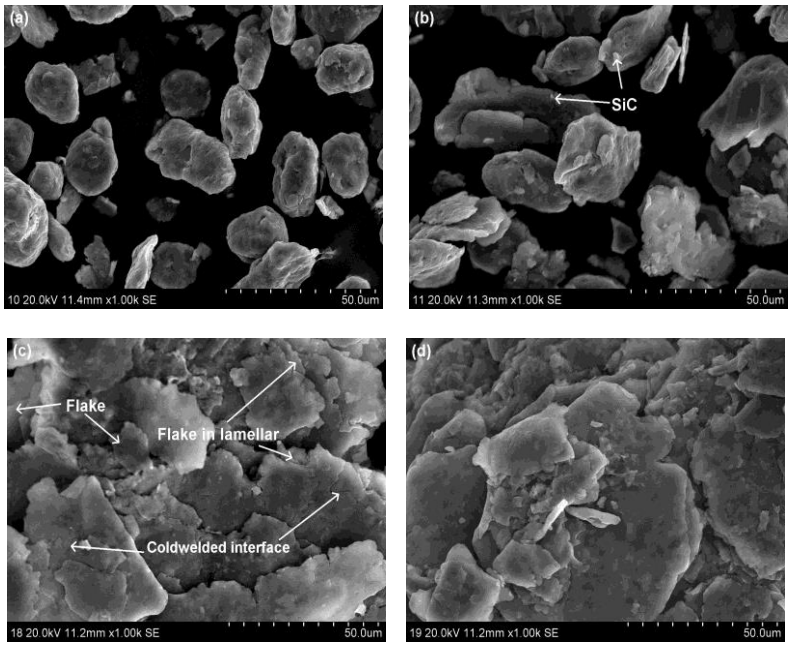

Fig. 2 SEM morphology of SiC_p/Al composites (2.5 wt%) for (a) 12h, (b) 18h, (c) 24h and (d) 30 h of *milling time in the as-milled condition.*

Distribution of SiC_p in the Al matrix was examined using the optical microscopy and SEM equipped with EDS. Optical microscopy images of the sintered SiC_p/Al composites with different SiC_p contents for balling time of 24 h are shown in Fig. 3 (a), (c), (e) and (g). And EDS mapping of the corresponding composites is shown in Fig. 3 (b), (d), (f) and (h). It can be observed that the distribution of SiC_p in the composites is relatively homogeneous when the content of SiC_p is small (such as 1.5 wt% and 2.5 wt%), as shown in Fig. 3 (a) , (b), (c) and (d). However, it is evident that the distribution of SiC_p in the composite is not uniform and the local aggregation of SiC_p in the composites is visible when the SiC_p content is above 3.5 wt% (see Fig. 3 (e), (f), (g) and (f)). It is possible to effect the mechanical properties of the composites.

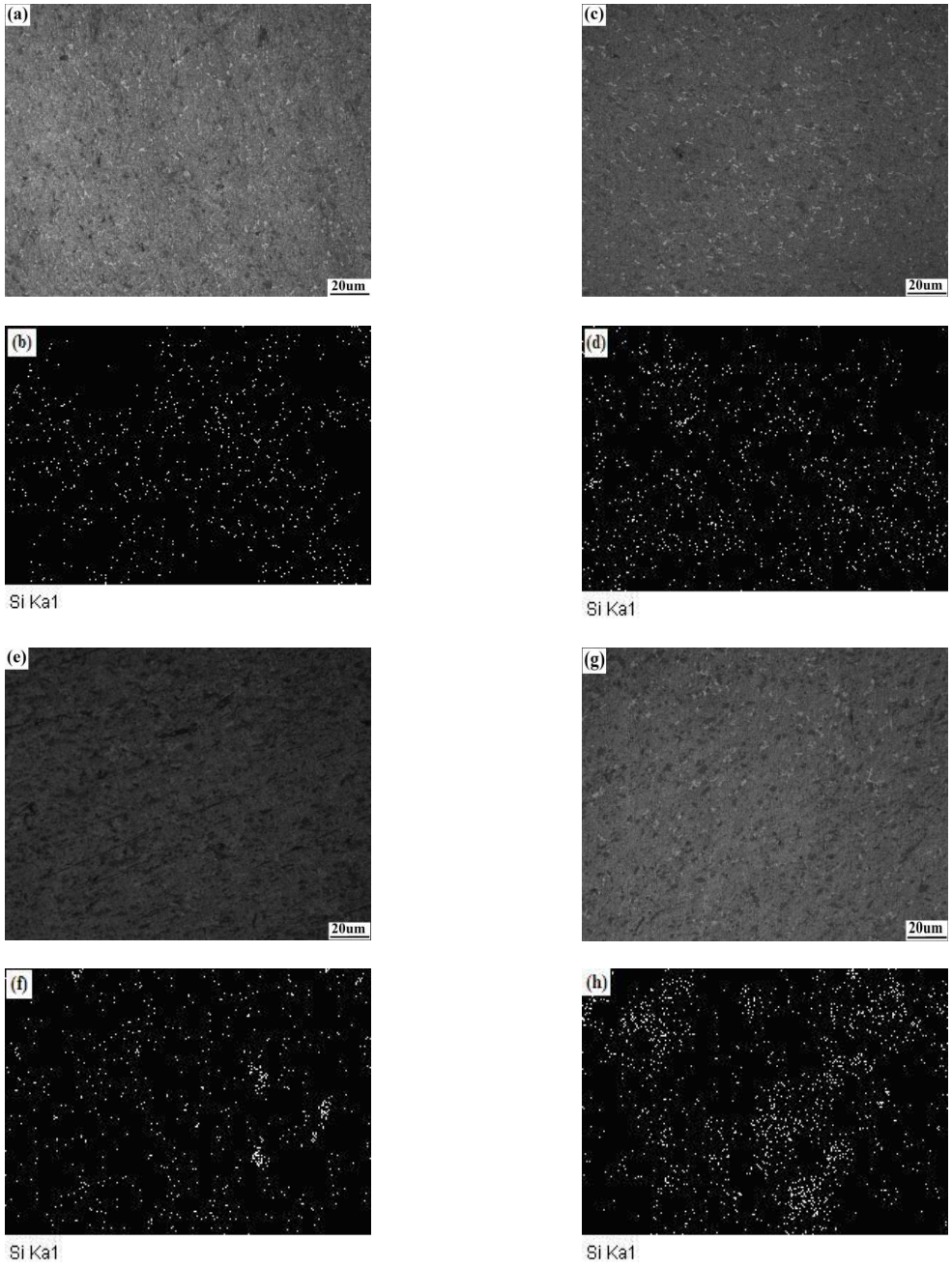

Fig. 3. Distribution of SiC_p in the sintered SiC_p/Al composites with different SiC_p contents for 24 of milling time, (a, b) 1.5 wt%; (c, d) 2.5 wt%; (e, f) 3.5 wt%, (g, h) 4.5 wt%.

In X-ray diffractograms aluminum and silicon carbide peaks were observed for 2.5 wt%-SiC_p/Al composites, as shown in Fig. 4. Pure aluminum gives 2*è* peaks at 37º-39º, 44º-46º, 64.5º-66.5º, 78º-79º and 82º-83º. The formation of new 2*è* peaks at 34º-35º, 35.5º-36.5º, 60º and 71.5º-72º which confirms the presence of SiC_p in the composite powder.

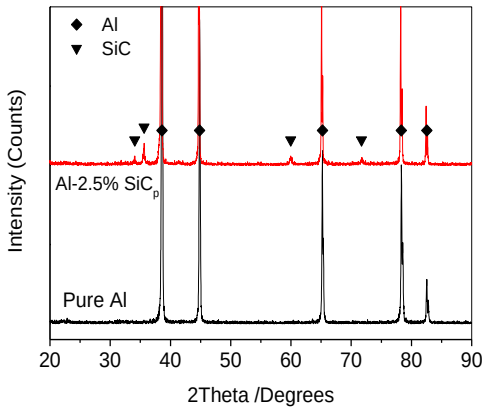

Fig. 4. XRD of pure aluminum and SiC_p/Al composite.

3.2 Mechanical Properties

Vickers hardness values were measured. The hardness results from the pure aluminum and SiC_p/Al composites samples are summarized in Fig. 5. It has been observed that the hardness of composites is invariably higher than that of the pure Al. This effect is attributed to the presence of hard SiC_p, which aid to the load bearing capacity of the material and also restricts the matrix deformation by constraining dislocation movement [11]. It is also believed that since SiC particles are harder than pure Al, their inherent property of hardness is rendered to the soft matrix [12,13]. With the increase of the SiC_p contents, the hardness of the composites increases initially and decreases later. The maximum of hardness is obtained at the SiC_p content of 2.5 wt.%. The hardness of pure aluminum sample was 64.0±3.2 HV, while the hardness of 2.5 wt.% SiC_p reinforced aluminum matrix composites was 80.5 ± 4.03 HV, showing 25.8% increments over the unreinforced aluminum under otherwise identical experimental conditions. It can be explained that fine size SiC_p can inhibit grain growth in aluminum matrix through grain boundary pinning and therefore lead to a finer grain structure of aluminum. This results in many inhibition sites for the movement of dislocations leading to increased hardness value. Moreover, the significant difference in coefficient of thermal expansion of Al matrix and SiC_p can result in the high dislocation density in composites which would have caused the increase in the hardness. However, with increasing SiC_p content up to 3.5 wt%, the agglomeration of SiC_p appears shown in Fig. 3 (f) and (h), which in turn degraded the hardness of the SiC_p/Al composites.

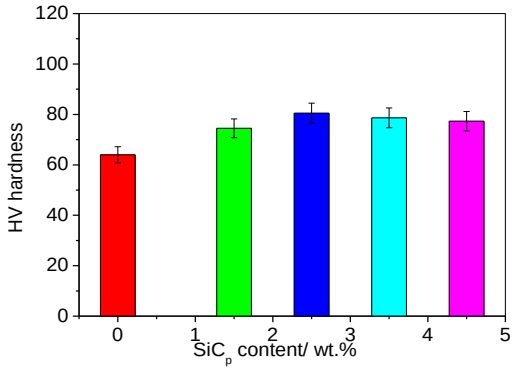

Fig. 5 The Vickers hardness of the pure aluminum and SiC_p/Al composite specimens.

Tensile properties of SiC_p /Al composites with different SiC_p contents are shown in Fig. 6. Fig. 6 (a) shows the representative engineering stress-strain curves of the SiC_p /Al composites with different SiC_p contents. The curves have four typical stages: (1) elastic loading up to the yielding point, (2) substantial strain hardening (3), a "steady state" regime where the flows tress remains almost constant for the remaining deformation toward the peak stress, (4) elongation after reaching peak stress until final fracture. Fig. 6 (b) shows the relationship of ultimate tensile strength (UTS) and elongation to fracture (δ) of the SiC_p /Al composites with different SiC_p contents. When the SiC_p content is 2.5 wt%, the UTS of the composites reach the maximum value. The composites with an addition of 1.5 and 2.5 wt. % SiC_p possess UTS of 171.8 and 177.3 MPa, respectively, which are 37.1% and 41.5% enhancement over the aluminum matrix sample (125.3 MPa). The same strong improvement of tensile strength is seen in the SiC_p/Al composite [14]. Carreno et al. [15] believed that due to difference of the thermal co-efficient of expansion between matrix and the homogeneously dispersed SiC_p particles, the high dislocation density is induced and particles work as the barriers for dislocation movement. The interaction of dislocations with the non-shearable particles increases the strength level of composite samples.

In contrast, the effect of larger content (3.5 wt% and 4.5 wt%) of SiC_p on tensile strength was adverse. The tensile strength decreased with the increase in SiC_p content. The reason was attributed to the formation of clusters in the two composites (as shown in Fig. 3 (f) and (h)). On one hand, voids might exist in clusters, which act as microcrack sources. On the other hand, reinforcement clusters induced stress concentration and accelerated the propagation of cracks [16,17]. As also shown in Fig. 6 (b), the elongation of SiC_p/Al composite decreased from 12.3% of pure aluminum to 7.0% of SiC_p/Al composite with 4.5 wt% SiC_p. It resulted from higher triaxial stress state caused by the increase of clusters and the reduction of the interparticle distance. Many researchers reported that the introduction of the SiC particles increases tensile strength but decreases the ductility and toughness of the aluminum matrix composites [18-21]. It is also noted that the trend of UST and elongation in present study is consistent with the conclusions reported in the literatures.

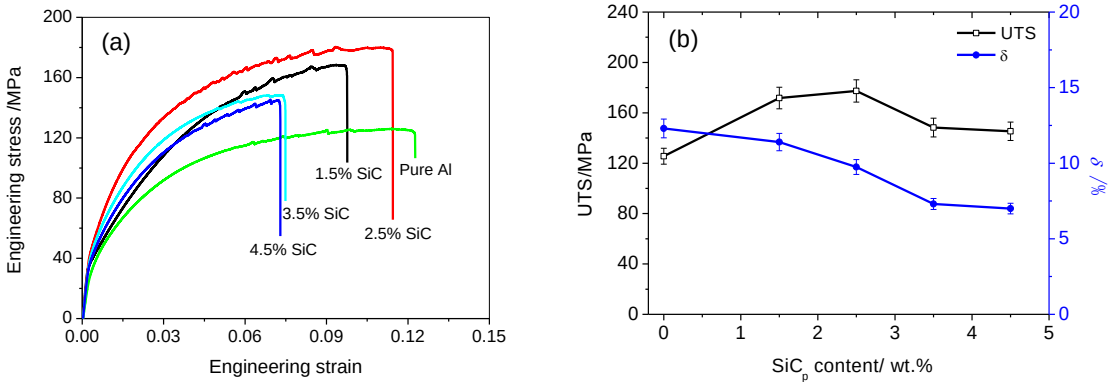

Fig. 6. Tensile properties of SiC_p/Al composites with different SiC_p contents. (a) stress-strain curves; (b) relationship of UTS and δ with the SiC_p content

The fractured surfaces of the composites tested are shown in Fig. 7. As shown in Fig. 7 (a), it can be seen that dimples and tear ridges are tiny and uniform with distinguishing feature of obvious trend along the loading direction of tensile stress, indicating a the ductile fracture for pure Al. Fig. 7(b) and (c) show the fractographes of composites with the addition of 1.5 wt. % and 2.5 wt. % SiC_p. The fracture mode of the composites is ductile fracture, which is consistent to the elongation data. The obvious tearing ridge line and ductile dimples on the fracture surface can be also observed, which is in accordance with a superior combination of strength and ductility.

Fig. 7 (d) and (e) show the fractographs of Al matrix composites with the addition of 3.5 wt. % and 4.5 wt. % SiC_p. The difference in fracture morphology is mainly due to the different particle dispersion states. It can be seen from Fig. 7 (d) and (e) that the SiC particles distribute inhomogeneously. This particle agglomeration is especially serious in Fig. 7 (e). This is consistent to tensile properties (in Fig. 6), which indicates that non-uniform particle distribution cannot fully reinforce the matrix alloy because the particle-rich region can prevent the crack propagation effectively but the particle-poor region offers channels for crack propagation [22]. Furthermore, it can be found from Fig. 7 (d) and (e) that there are many dispersed micropores in composites, caused by the poor combination among aluminum particles with the increase in the amount of SiC particles. The micropores are deterioration of mechanical properties of the composite because they offer channel for crack propagation. The fracture of the SiC_p/Al composites with larger content of SiC_p change into brittle fracture.

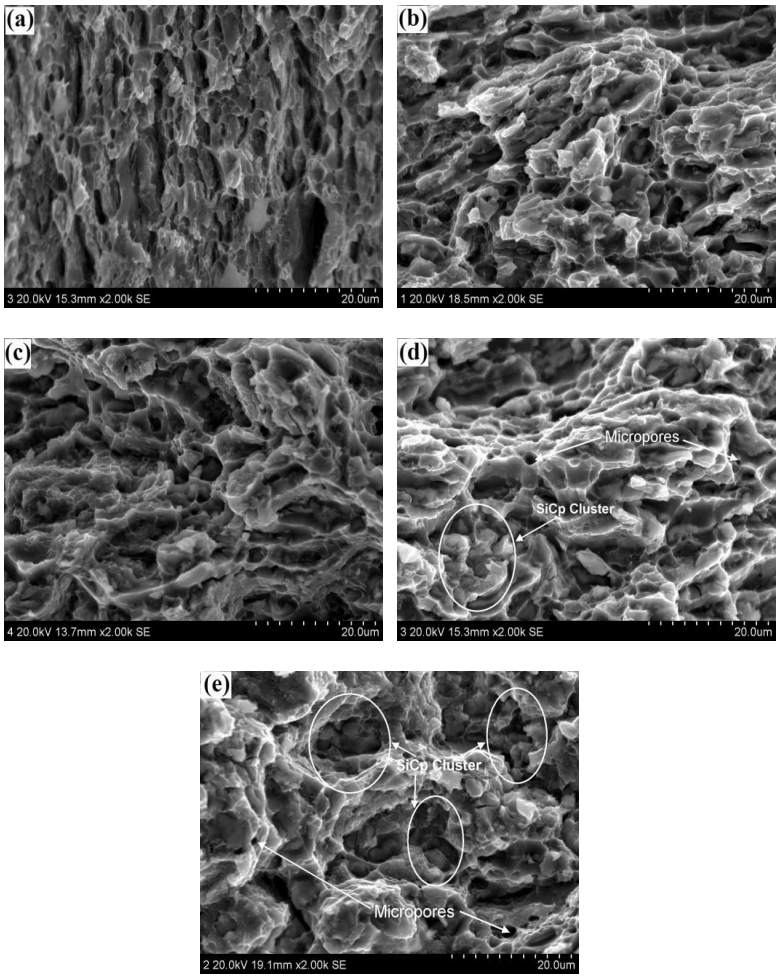

Fig. 7. Tensile fracture images of (a) Pure Al, (b) 1.5 wt%, (c) 2.5 wt%, (d) 3.5 wt%, (e) 4.5 wt%. composites.

4. Conclusions

SiC_p/Al composites were successfully fabricated through the powder metallurgy technique. The microstructure and mechanical properties were investigated. The main conclusions can be drawn as follows: The micro-sized SiC particles are dispersed homogeneously in the aluminum matrix when the content of SiC_p is up to 2.5 wt%.

Compared to the unreinforced aluminum matrix, the addition of 2.5 wt.% of SiC_p raises the UTS from 125.3 to 177.3 MPa, i.e. by about 41.5%. Different strengthening mechanisms contributed to the obtained strength and hardness improvements including grain refinement, accommodation of CTE mismatch between the matrix and the particles, and the load bearing effects. The fracture mechanism changes from ductile to brittle with increasing the SiC particles contents.

Acknowledgements

This work is supported by the Natural Science Foundation of Liaoning (2015602642), Scientific Fund of Liaoning Provincial Education Department and research project of application technology on Shenyang science and technology talent.

References

[1] Y. Sumankant, C. S. Jawalkar, A. S. Verma, N.M.Suri, Mater. Today: Proc. **4**, 2927 (2017).
[2] A. P. Reddy, P. V. Krishna, R. N. Rao, N. V. Murthy, Mater. Today: Proc. **4**, 3959 (2017).
[3] T. P. D. Rajan, R. M. Pillai, B. C. Pai, K. G. Satya Narayana, P. K. Rohatgi, Compos. Sci. Technol. **67**, 3369 (2007).
[4] S. W. Lai, D. D. L. Chung, J. Mater. Chem. **6**, 469 (1996).
[5] J. Hashim, L. Looney, M. S. J. Hashmi, J. Mater. Process. Technol. **92–93**, 1 (1999).
[6] M Kok, J. Mater. Process. Technol. **161**, 381 (2005).
[7] A. M. Murphy, S. J. Howard, T. W. Clyne, Mater. Sci. Technol. 14, **959** (1998).
[8] Y. Yang, J. Lan, X. Li, Mater. Sci. Eng. A **380**, 378 (2004).
[9] L. Kollo, M. Leparoux, C. R. Bradbury, C. Jaggi, C. M. Efraín, R. A. Mikel, J. Alloys Compd. **489**, 394 (2010).
[10] Z. Y. Liu, Q. Z. Wang, B. L. Xiao, Z. Y. Ma, Y. Liu, Mater. Sci. Eng. A **527**. 5582 (2010).
[11] A. Mazahery, M. O. Shabani, J. Compos. Mater. **45**, 2579 (2011).
[12] P. S. Cooke, P. S. Werner, Mater. Sci. Eng. A **144**, 189 (1991).
[13] D. P. Mondal, N. V. Ganesh, V. S. Muneshwar, Mater. Sci. Eng. A **433**, 18 (2006).
[14] F. Tang, M. Hagiwara, J. M. Schoenung, Mater. Sci. Eng. A **407**, 306 (2005).
[15] C. Carreno Gallardo, I. Estrada Guel, C. Lopez Melendez, R. Martinez Sanchez, J. Alloys Compd. **586**, S68 (2014).
[16] A. Slipenyuk, V. Kuprin, Y. Milman, J. E. Spowart, D. B. Miracle, Mater, Sci. Eng. A **381**, 165 (2004).
[17] A. Slipenyuk, V. Kuprin, Y. Milman, V. Goncharuk, J. Eckert, Acta Mater. 54 157 (2006).
[18] R. G. Reddy, Rev. Adv. Mater. Sci. **5**, 121 (2003).
[19] Y. C. Kang, S. L. I. Chen, Chem. Phys. **85**, 438 (2004).
[20] A. Mazahery, M. O. Shabani, J. Mater. Eng. Perform **21**, 247 (2012).
[21] S. M. Zebarjad, S. A. Sajjadi, Mater. Des. **28**, 2113 (2007).
[22] L. N. Guan, L. Geng, H.W. Zhang, W. Ren, J. Wuhan Univ. Technol. **24**, 13 (2009).